Space-Time Discontinuous Galerkin Methods for Compressible Flows

Part III Efficient Solution Techniques

Jaap van der Vegt

Numerical Analysis and Computational Mechanics Group
Department of Applied Mathematics
University of Twente
The Netherlands

Montreal Scientific Computing Days

April 30 - May 2, 2008

Introduction

- The space-time discretization of the Navier-Stokes equations results in very large systems of coupled algebraic equations which need to be solved each time step.
- Efficient solution techniques should preserve the locality of the DG discretization, which is accomplished using
  - optimized Runge-Kutta pseudo-time integration methods
  - multigrid techniques

Overview of Lecture

- Space-time discretization of advection-diffusion equation
- Pseudo-time integration methods for space-time discontinuous Galerkin discretizations
- Multigrid techniques
- Applications
- Concluding remarks

Efficient Solution of Nonlinear Algebraic System

- The space-time DG discretization results in a large system of nonlinear algebraic equations:

$$\mathcal{L}(\hat{U}^n; \hat{U}^{n-1}) = 0$$

- This system is solved by marching to steady state using pseudo-time integration and multigrid techniques:

$$\frac{\partial \hat{U}}{\partial \tau} = -\frac{1}{\Delta t}\mathcal{L}(\hat{U}; \hat{U}^{n-1})$$

Benefits of Coupled Pseudo-Time and Multigrid Approach

- The locality of the DG discretization is preserved, which is beneficial for parallel computing and hp-adaptation.
- In comparison with a Newton method the memory overhead is considerably smaller
- The algorithm has good stability and convergence properties and is not sensitive to initial conditions

EXI Runge-Kutta Scheme

- **Explicit Runge-Kutta method for inviscid flow with Melson correction.**

  1. Initialize $\hat{V}^0 = \hat{U}$.
  2. For all stages $s = 1$ to 5 compute $\hat{V}^s$ as:

  $$\big(I + \alpha_s \lambda I\big)\,\hat{V}^s = \hat{V}^0 + \alpha_s \lambda \big(\hat{V}^{s-1} - \mathcal{L}(\hat{V}^{s-1}; \hat{U}^{n-1})\big).$$

  3. Return $\hat{U} = \hat{V}^5$.

- Runge-Kutta coefficients: $\alpha_1 = 0.0791451$, $\alpha_2 = 0.163551$, $\alpha_3 = 0.283663$, $\alpha_4 = 0.5$ and $\alpha_5 = 1.0$.

- The factor λ is the ratio between the pseudo- and physical-time step: $\lambda = \Delta\tau/\Delta t$.

EXV Runge-Kutta Scheme

- **Explicit Runge-Kutta method for viscous flows.**

  1. Initialize $\hat{V}^0 = \hat{U}$.
  2. For all stages $s = 1$ to 4 compute $\hat{V}^s$ as:

$$\hat{V}^s = \hat{V}^0 - \alpha_s \lambda \mathcal{L}(\hat{V}^{s-1}; \hat{U}^{n-1}).$$

  3. Return $\hat{U} = \hat{V}^4$.

- Runge-Kutta coefficients: $\alpha_1 = 0.0178571$, $\alpha_2 = 0.0568106$, $\alpha_3 = 0.174513$ and $\alpha_4 = 1.0$.

EXI-EXV Runge-Kutta Scheme

- Time accuracy is not important in pseudo-time, we apply therefore local pseudo-time stepping and deploy whichever scheme gives the mildest stability constraint.
- The EXI scheme has the mildest stability constraint for relatively high cell Reynolds numbers and the EXV scheme for relatively low cell Reynolds numbers.
- The pseudo-time Runge-Kutta schemes act as smoother in a multigrid algorithm.

Advection-Diffusion Equation

- Consider the time-dependent scalar advection-diffusion equation:

$$\begin{cases} u_t + a u_x - d u_{xx} = 0, \\ u(x,0) = u_0, \\ \text{periodic boundary conditions} \end{cases}$$

- The flow domain $\mathcal{E}_h = \mathbb{R} \times \mathbb{R}^+$, restricted to the time interval (t^n, t^{n+1}), has a tessellation $\mathcal{T}_h^n$ consisting of uniform elements $\mathcal{K} = (x_j, x_{j+1}) \times (t^n, t^{n+1})$ with $j \in \mathbb{Z}$ and $n \in \mathbb{N}$.

- The corresponding function space is:

$$V_h^k \equiv \{ w \in L^2(\mathcal{E}_h) : w|_{\mathcal{K}} \circ G_{\mathcal{K}} \in P^m(\hat{\mathcal{K}}), \quad \forall \mathcal{K} \in \mathcal{T}_h^n \}$$

Space-time Discretization

- The weak formulation is equal to: Find a $u_h \in V_h^k$, such that for all $w \in V_h^k$:

$$
\begin{aligned}
&-\sum_{\mathcal{K}\in\mathcal{T}_h^n}\int_{\mathcal{K}}\Big(\frac{\partial w}{\partial t}u_h+\frac{\partial w}{\partial x}(au-d(\frac{\partial u_h}{\partial x}-\mathcal{R}))\Big)\,d\mathcal{K}\\
&+\sum_{K\in\mathcal{T}_h^n}\Big(\int_{K(t_{n+1}^-)}w^L u_h^L\,dK-\int_{K(t_n^+)}w^L u_h^R\,dK\Big)\\
&+\sum_{\mathcal{S}\in\mathcal{S}_I^n}\int_{\mathcal{S}}[\![w]\!](a\widehat{u_h}-d\{\!\{\frac{\partial u_h}{\partial x}-\eta\mathcal{R}^{\mathcal{S}}\}\!\})\,d\mathcal{S}=0,
\end{aligned}
$$

where standard upwinding is used for the numerical flux $a\widehat{u_h}$.

Lifting Operator

- The local lifting operator $\mathcal{R}^{\mathcal{S}} \in \mathbb{R}$ is defined as:

$$\sum_{\mathcal{K} \in \mathcal{T}_h^n} \int_{\mathcal{K}} w \mathcal{R}^{\mathcal{S}} \, d\mathcal{K} = \int_{\mathcal{S}} \{\!\{ w \}\!\} [\![u_h]\!] \, d\mathcal{S} \quad \text{for } \mathcal{S} \in \mathcal{S}_I^n,$$

with global lifting operator $\mathcal{R} = \sum_{\mathcal{S} \in \mathcal{S}_I^n} \mathcal{R}^{\mathcal{S}}$.

- For stability of the discretization we take $\eta = 2$.

- More details on the derivation and analysis of the space-time discretization for the advection=diffusion equation, including a full hp-error analysis can be found in:

  J.J. Sudirham, J.J.W. van der Vegt, R.M.J. van Damme, Space-time discontinuous Galerkin method for advection-diffusion problems on time-dependent domains, *Applied Numerical Mathematics*, **56** (2006) 1491-1518.

Discrete System

- Using the linear polynomial expansion of u_h and w yields a discrete system the expansion coefficients $\hat{u}$ of u_h at time level n:

$$\mathcal{L}_h(\hat{u}^n; \hat{u}^{n-1}) \equiv (\mathcal{L}_h^a + \mathcal{L}_h^d)\hat{u}^n + \mathcal{L}_h^t \hat{u}^{n-1} = 0$$

- This $3\mathbb{Z} \times 3\mathbb{Z}$ system has a block Toeplitz structure with 3×3 blocks and its stencil has the form:

$$\mathcal{L}_h \cong \left[L_h \quad \middle| \quad D_h \quad \middle| \quad U_h \right],$$

where L_h represents the left block, D_h the diagonal block and U_h the right block.

Advective Part

- The advective part $\mathcal{L}_h^a$ of the discretization depends on the Courant number

$$\sigma = \frac{a\Delta t}{h},$$

and gives the following block tridiagonal contribution to the system:

$$\mathcal{L}_h^a \cong \left[\begin{array}{ccc|ccc|ccc} -\sigma & -\sigma & \sigma & 1+\sigma & \sigma & -\sigma & 0 & 0 & 0 \\ \sigma & \sigma & -\sigma & -\sigma & \frac{1}{3}+\sigma & \sigma & 0 & 0 & 0 \\ \sigma & \sigma & -\frac{4}{3}\sigma & -2-\sigma & -\sigma & 2+\frac{4}{3}\sigma & 0 & 0 & 0 \end{array}\right].$$

- The right block is zero because the advective numerical flux is upwind ($a > 0$).

Diffusive Part

- The diffusive part $\mathcal{L}_h^d$ depends on the Courant number, the stabilization constant η and the cell Reynolds number:

$$\mathrm{Re}_h = \frac{ah}{d},$$

and gives a block tridiagonal contribution to the system:

$$\mathcal{L}_h^d \cong \frac{\sigma}{\mathrm{Re}_h}\left[\begin{array}{ccc|ccc|ccc} -2\eta & 1-2\eta & 2\eta & 4\eta & 0 & -4\eta & -2\eta & -1+2\eta & 2\eta \\ -1+2\eta & -2+2\eta & 1-2\eta & 0 & 4\eta & 0 & 1-2\eta & -2+2\eta & -1+2\eta \\ 2\eta & -1+2\eta & -\frac{13}{6}\eta & -4\eta & 0 & \frac{13}{3}\eta & 2\eta & 1-2\eta & -\frac{13}{6}\eta \end{array}\right],$$

with the Von Neumann number defined as $\delta = \frac{\sigma}{\mathrm{Re}_h}$.

Coupling Term

- The contribution $\mathcal{L}_h^t$ related to the previous space-time slab is block diagonal:

$$\mathcal{L}_h^t \cong \left[\begin{array}{ccc|ccc|ccc} 0 & 0 & 0 & -1 & 0 & 0 & 0 & 0 & 0 \\ 0 & 0 & 0 & 0 & -\frac{1}{3} & 0 & 0 & 0 & 0 \\ 0 & 0 & 0 & 2 & 0 & 0 & 0 & 0 & 0 \end{array}\right].$$

Pseudo-Time Algorithm

- The pseudo-time algorithm for the advection-diffusion equation is then equal to

$$\frac{\partial \hat{u}^n}{\partial \tau} = -\frac{1}{\Delta t}((\mathcal{L}^a + \mathcal{L}^d)\hat{u}^n + \mathcal{L}^t \hat{u}^{n-1}).$$

- In the stability analysis, however, we only need to consider the transients

$$\frac{\partial \hat{u}^n}{\partial \tau} = -\frac{1}{\Delta t}(\mathcal{L}^a + \mathcal{L}^d)\hat{u}^n$$

Stability of the EXI and EXV method

- The stability analysis of the EXI and EXV method is similar and therefore treated simultaneously.

- The vector of expansion coefficients in element j is assumed to be a Fourier mode:

$$\hat{u}_j^n = \hat{u}^F \exp(\imath\theta j)$$

  with $\hat{u}^F$ the amplitude of the mode, $\imath = \sqrt{-1}$ and $\theta \in (-\pi, \pi]$.

- With this assumption, the Fourier transform of the discrete system becomes:

$$\widehat{\mathcal{L}}(\theta) = L \exp(-\imath\theta) + D + U \exp(\imath\theta),$$

  with L the block-lower, D the block-diagonal and U the block-upper part of the matrix.

- The matrix $\widehat{\mathcal{L}}(\theta)$ is non-singular and can be diagonalized as

$$\widehat{\mathcal{L}}(\theta) = QMQ^{-1}$$

with Q the matrix of right eigenvectors and M the diagonal matrix with (complex) eigenvalues $\mu_i(\theta)$ with $i = 1, 2, 3$.

- Introducing $w = Q^{-1}\hat{u}^n$, reduces the pseudo-time equation to

$$\frac{\partial w_i}{\partial \tau} = -\frac{\mu_i(\theta)}{\Delta t} w_i, \quad \text{for } i = 1, 2, 3.$$

- Consider the generic scalar model problem of the form:

$$\frac{\partial w}{\partial \tau} = -\frac{\mu}{\Delta t} w,$$

where w and μ can be any of the three components of the corresponding vectors.

- Applying the EXI method to this model equation, the Runge-Kutta stages w^s are computed as

$$(1 + \alpha_s^i \lambda) w^s = w^0 + \alpha_s^i \lambda (1 - \mu)\, w^{s-1},$$

with $\lambda = \Delta\tau / \Delta t$

- The EXV method gives

$$w^s = w^0 - \alpha_s^v \lambda \mu\, w^{s-1}.$$

- The relation between two consecutive pseudo-time steps can be written in generic form as

$$w^n = G(-\lambda\mu)w^{n-1},$$

with G the algorithm dependent amplification factor.

- Starting with an initial condition w^{init}, we obtain after n steps

$$w^n = G(-\lambda\mu)^n w^{\text{init}}.$$

- In stability analysis, we are interested in the behavior of a perturbation of the initial condition.

- Due to linearity, the amplification of the perturbation is the same as the amplification of w.
- Clearly, the perturbation is bounded if $\|G^n\|$ is bounded, where $\|\cdot\|$ denotes the Euclidian (or discrete l_2) norm.
- A sufficient condition for stability is that the values $-\lambda\mu_i(\theta)$ for $i = 1, 2, 3$ and $\theta \in (-\pi, \pi]$ all lie inside the stability domain S given by

$$S = \{z \in \mathbb{C} \, : \, |G(z)| \leq 1\}.$$

- The discretization of the advection-diffusion equation only depends on the Courant number σ, the Von Neumann number δ and the constant η.
- For given values of these numbers, the factor λ of the Runge-Kutta algorithm should be chosen such that $-\lambda\mu_i(\theta)$ lies inside the stability domain S.
- Once a suitable λ is found, it is convenient to express the stability in terms of the **pseudo-time Courant and Von Neumann numbers**

$$\sigma_{\Delta\tau} = \lambda\sigma \quad \text{and} \quad \delta_{\Delta\tau} = \lambda\delta$$

- Hence, for stability, the pseudo-time step $\Delta\tau$ must satisfy the Courant-Friedrichs-Levy (CFL) condition and the Von Neumann condition

$$\Delta\tau \leq \Delta\tau^a \equiv \frac{\sigma_{\Delta\tau}\Delta x}{a} \quad \text{and} \quad \Delta\tau \leq \Delta\tau^d \equiv \frac{\delta_{\Delta\tau}(\Delta x)^2}{d}.$$

We distinguish between flow regimes by introducing the *cell* Reynolds number, defined as:

$$\mathrm{Re}_{\Delta x} \equiv \frac{a\Delta x}{d}.$$

Stability Analysis

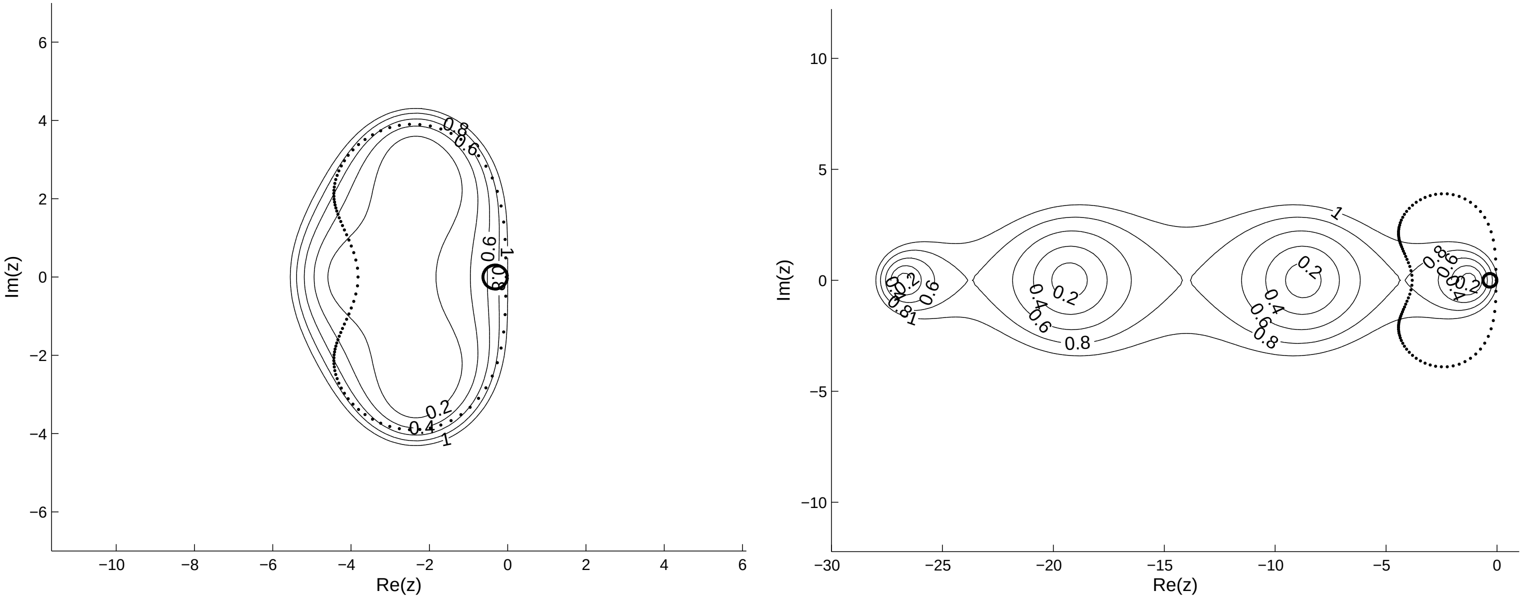

Stability domain and values $-\lambda\mu$ (dots) for the EXI method (L) and EXV method (R) in the steady-state inviscid flow regime with $\lambda = 1.8 \cdot 10^{-2}$. Pseudo-time CFL number is 1.8 and for this constraint only the EXI method is stable.

Stability Analysis

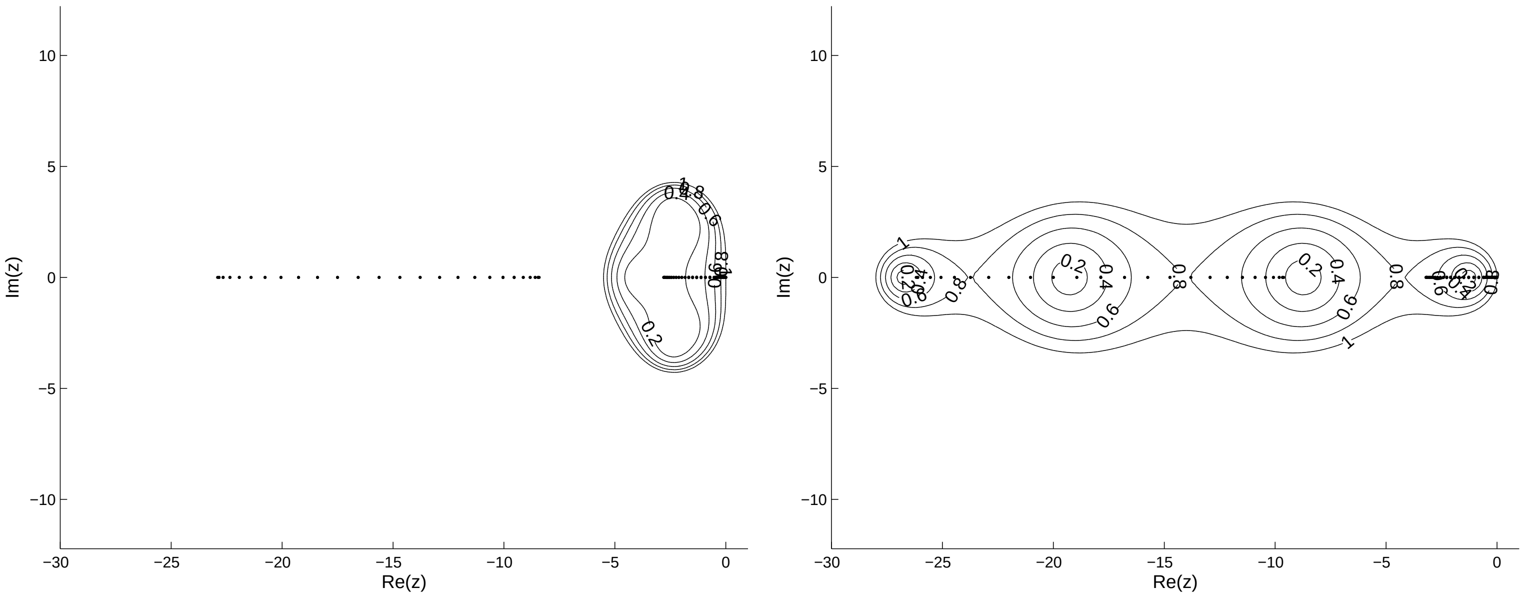

Stability domain and values $-\lambda\mu$ (dots) for the EXI method (L) and EXV method (R) in the steady-state viscous flow regime with $\lambda = 8 \cdot 10^{-5}$. The pseudo-time diffusion number is 0.8 and for this constraint only the EXV method is stable.

Stability Analysis

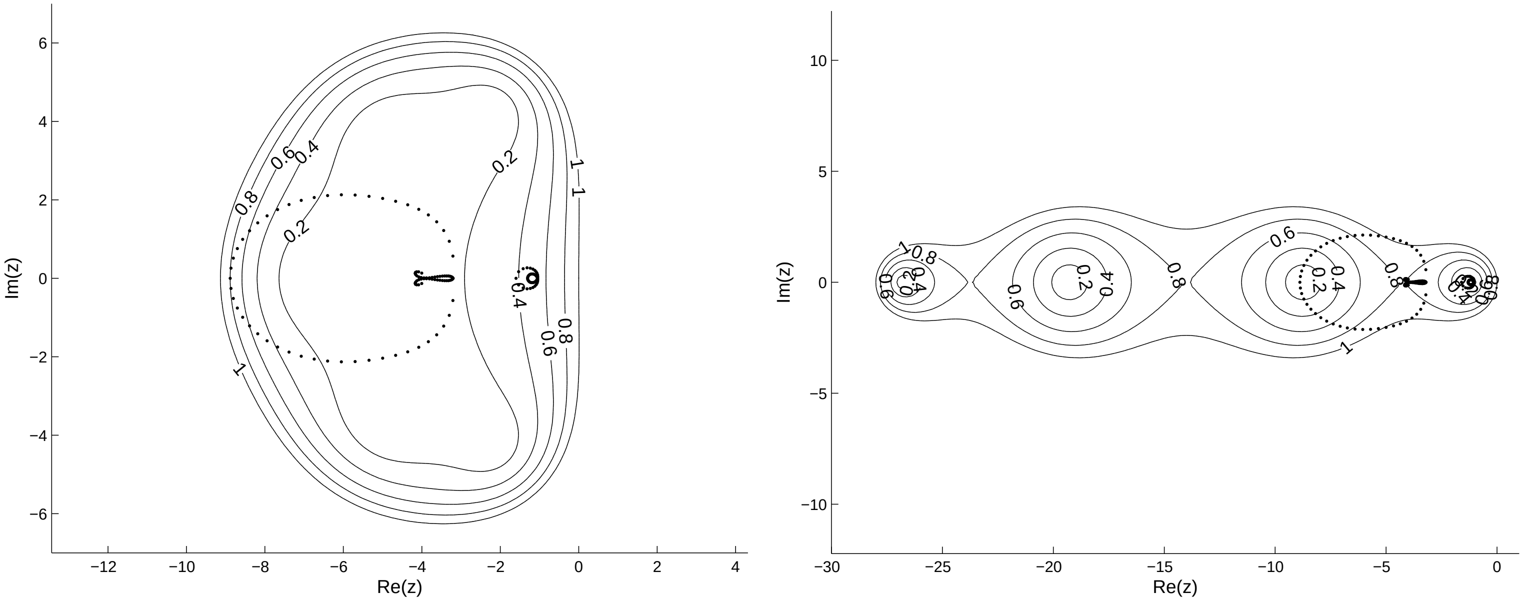

Stability domain and values $-\lambda\mu$ (dots) for the EXI method (L) and EXV method (R) in the time-dependent inviscid flow regime with $\lambda = 1.6$. The pseudo-time CFL number is 1.6 and for this constraint only the EXI method is stable.

Stability Analysis

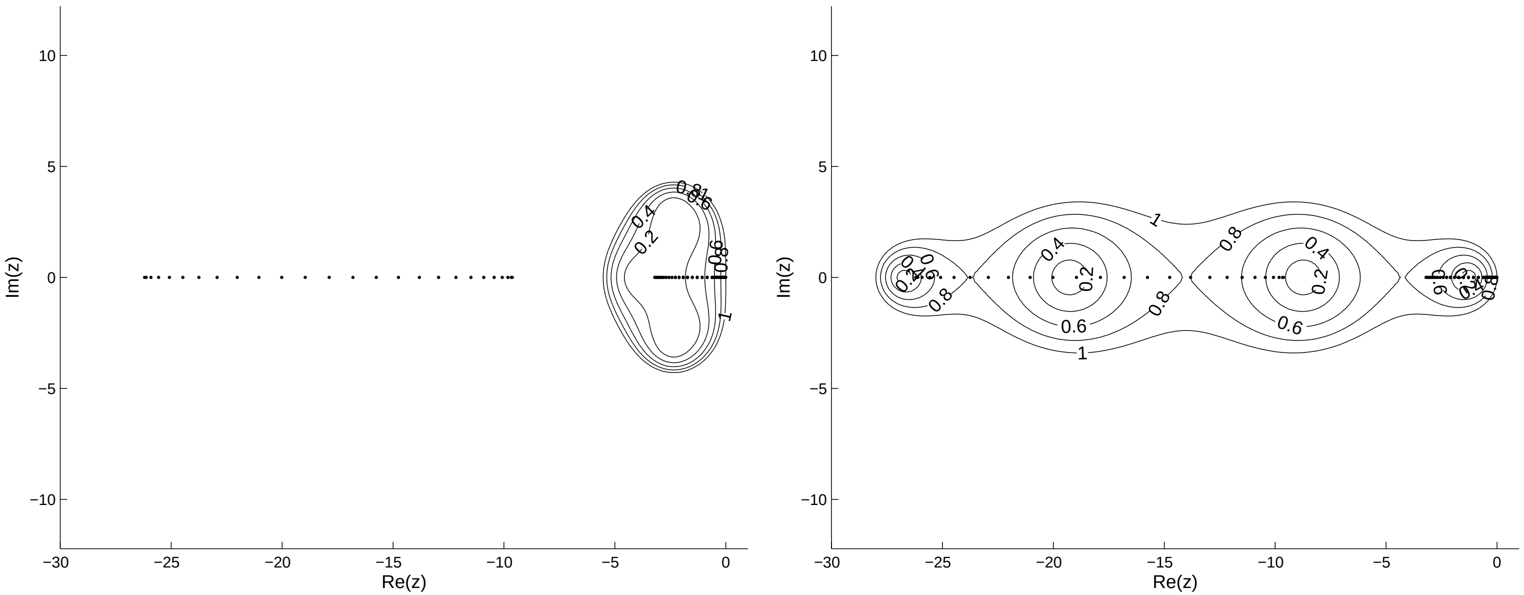

Stability domain and values $-\lambda\mu$ (dots) for the EXI method (L) and EXV method (R) in the time-dependent viscous flow regime with $\lambda = 8 \cdot 10^{-3}$. The pseudo-time diffusion number is 0.8 and for this constraint only the EXV method is stable.

Stability Analysis for Euler Equations

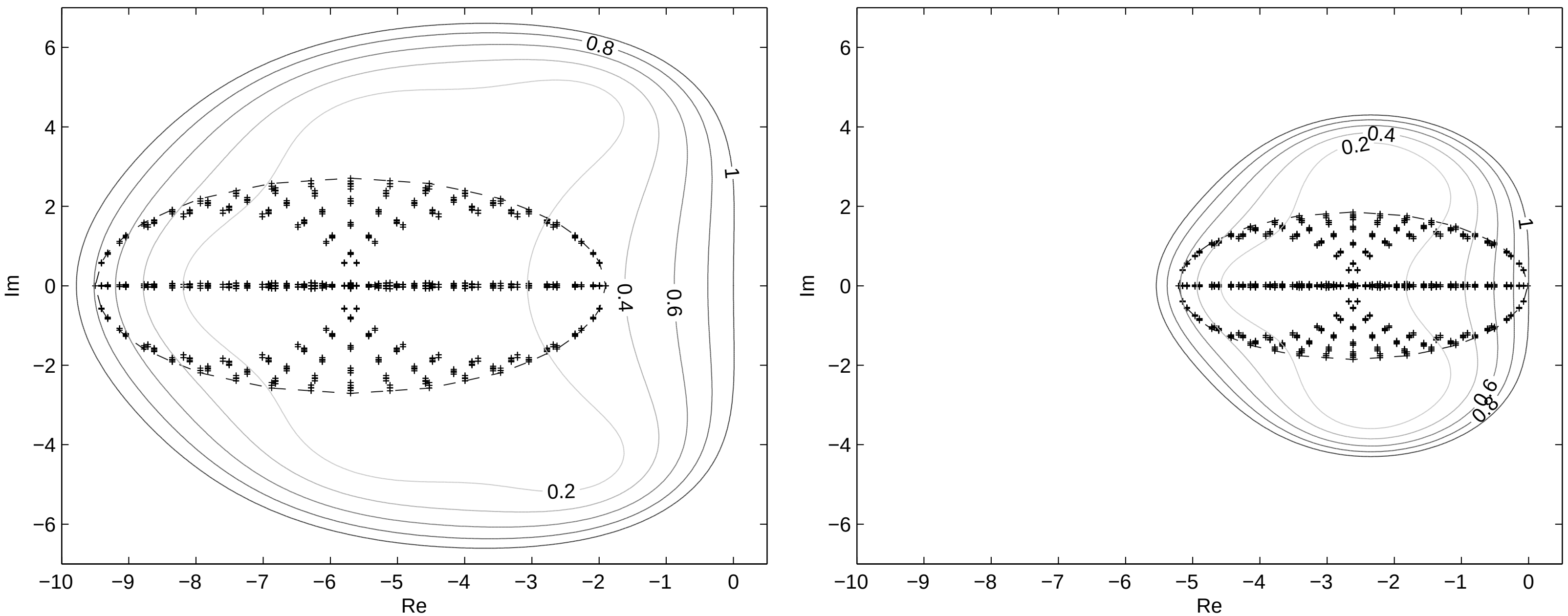

Stability domain of RK scheme and eigenvalues of linearized Euler equations.
$\sigma_{\triangle t} = 1$, $\sigma_{\triangle \tau} = 1.9$ (left), $\sigma_{\triangle t} = 100$, $\sigma_{\triangle \tau} = 1.3$ (right).

Performance of Time Integration Schemes

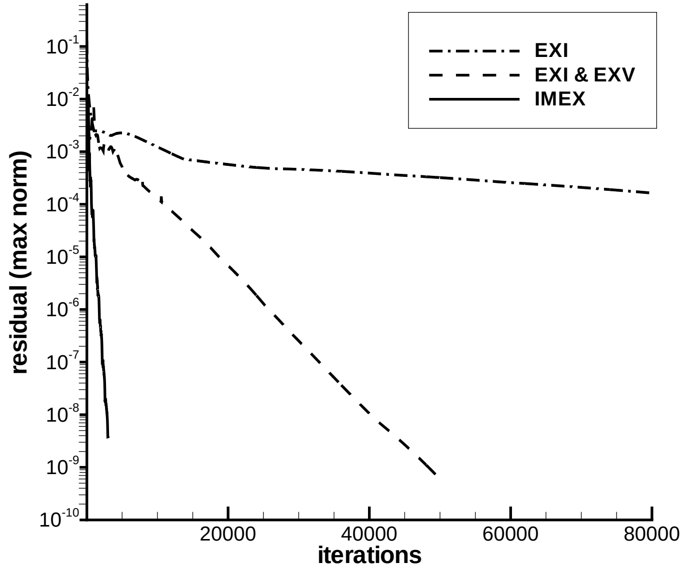

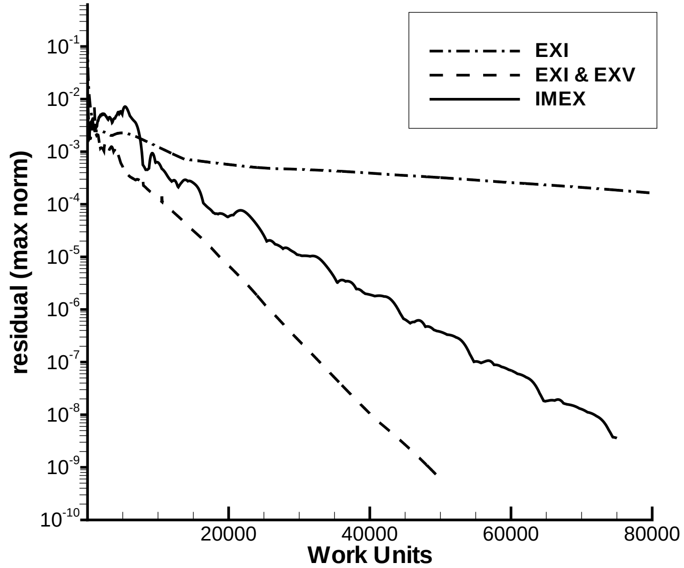

Convergence to steady state for the A1 case ($M_\infty = 0.8$, $Re_\infty = 73$, $\alpha = 12^\circ$) on a 112×38 grid in terms of iterations (L) and work units (R).

Performance of Time Integration Schemes

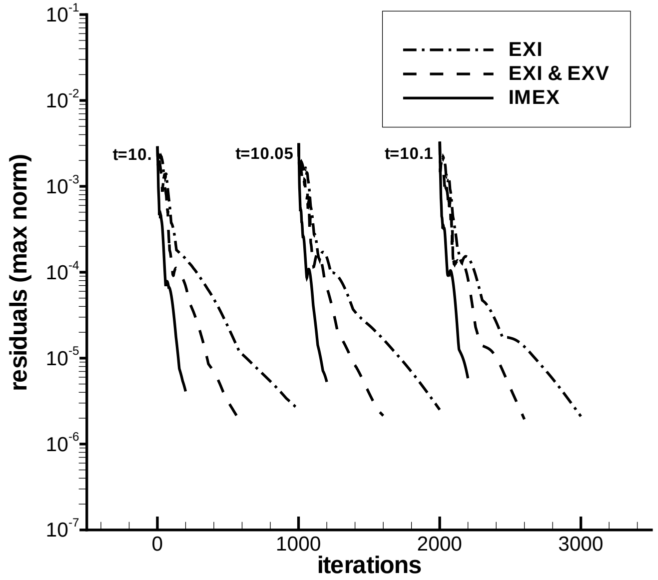

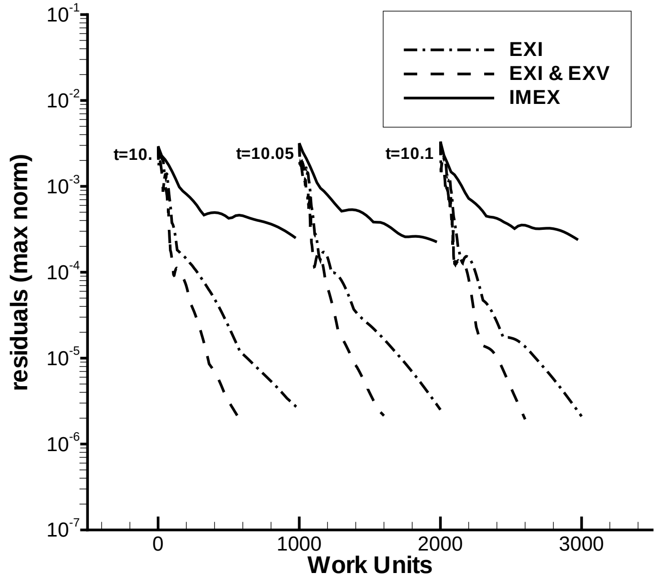

Convergence in pseudo-time for three physical time steps in the A7 case ($\mathrm{M}_\infty = 0.85$, $\mathrm{Re}_\infty = 10^4$, $\alpha = 0^\circ$) on a 224×76 grid, expressed in terms of iterations (top) and work units (bottom).

Two-level h-multigrid algorithm

- At the core of any multigrid method is the two-level algorithm.
- Subscripts $(\cdot)_h$ and $(\cdot)_H$ denote a quantity $(\cdot)$ on the fine and coarse grid.
- Define:
  - $\hat{U}$ an approximation of the solution $\hat{U}^n$
  - R the restriction operator for the solution
  - $\bar{R}$ the restriction operator for the residuals
  - P the prolongation operator
- The h-multigrid algorithm is applied only in space, hence the time-step is equal on both levels; but multi-time multi-space multigrid is also feasible.

Two-level h-multigrid algorithm

Two-level algorithm.

1. Take one pseudo-time step on the fine grid with the combined EXI and EXV methods, this gives the approximation $\hat{U}_h$.
2. Restrict this approximation to the coarse grid: $\hat{U}_H = R(\hat{U}_h)$.
3. Compute the forcing:

$$F_H \equiv \mathcal{L}(\hat{U}_H; \hat{U}_H^{n-1}) - \bar{R}\big(\mathcal{L}(\hat{U}_h; \hat{U}_h^{n-1})\big)\,.$$

4. Solve the coarse grid problem for the unknown $\hat{U}_H^*$:

$$\mathcal{L}(\hat{U}_H^*; \hat{U}_H^{n-1}) - F_H = 0,$$

5. Compute the coarse grid error $E_H = \hat{U}_H^* - \hat{U}_H$ and correct the fine grid approximation: $\hat{U}_h \leftarrow \hat{U}_h + P(E_H)$.

Two-level h-multigrid algorithm

- Solving the coarse grid problem at stage four of the multigrid algorithm can again be done with the two-level algorithm.
- This recursively defines the V-cycle multi-level algorithm in terms of the two-level algorithm.
- It is common practice to take ν_1 pseudo-time pre-relaxation steps at stage one and another ν_2 post-relaxation pseudo-time steps after stage five.
- The exact solution of the problem on the coarsest grid is not always feasible; instead one simply takes $\nu_1 + \nu_2$ relaxation steps.

Inter-grid transfer operators

- The inter-grid transfer operators stem from the L_2-projection of the coarse grid solution U_H in an element $\mathcal{K}_H$ on the corresponding set of fine elements $\{\mathcal{K}_h\}$.
- The solution U_h in element $\mathcal{K}_h$ can be found by solving:

$$\int_{\mathcal{K}_h} W_i U_i^h \, d\mathcal{K} = \int_{\mathcal{K}_h} W_i U_i^H \, d\mathcal{K}, \quad \forall W \in W_h.$$

- This relation supposes the embedding of spaces, i.e. $W_H \subset W_h$, to ensure that U_H is defined on $\mathcal{K}_h$.

Prolongation algorithm

- Introducing the polynomial expansions of the test and trial functions, we obtain the prolongation operator $P : U^H \to U^h$:

$$\hat{U}^h_{im} = (M_h^{-1})_{ml}\Big(\int_{\mathcal{K}_h} \psi^h_l \psi^H_n \, d\mathcal{K}\Big)\hat{U}^H_{in}.$$

  with the mass matrix M_h of element $\mathcal{K}_h$

- The restriction operator for the residuals is defined as the transpose of the prolongation operator: $\bar{R} = R^T$.

- The restriction operator R for the solution is defined as $R = P^{-1}$, such that the property $U_H = R(P(U_H))$ holds, meaning that the inter-grid transfer does not modify the solution.

Two-level Fourier analysis for a scalar advection-diffusion equation

- Consider the time-dependent scalar advection-diffusion equation:

$$\begin{cases} u_t + au_x - du_{xx} = 0, \\ u(x,0) = u_0, \\ \text{periodic boundary conditions} \end{cases}$$

- The discrete system for the expansion coefficients $\hat{u}$ of u at time level n in the space-time discretization can be expressed as

$$\mathcal{L}_h(\hat{u}^n; \hat{u}^{n-1}) \equiv (\mathcal{L}_h^a + \mathcal{L}_h^d)\hat{u}^n + \mathcal{L}_h^t \hat{u}^{n-1} = 0$$

- This $3\mathbb{Z} \times 3\mathbb{Z}$ system has a block Toeplitz structure with 3×3 blocks and its stencil has the form:

$$\mathcal{L}_h \cong \left[L_h \quad \middle| \quad D_h \quad \middle| \quad U_h \right],$$

where L_h represents the left block, D_h the diagonal block and U_h the right block.

Error amplification operator

- The error amplification operator of the two-level algorithm M_h^{TLA}, is given by:

$$M_h^{\mathrm{TLA}} = M_h^{\mathrm{CGC}} M_h^{\mathrm{REL}},$$

with M_h^{REL} the error amplification operator associated with either the EXI or the EXV scheme.

- The coarse grid correction (CGC) of the multigrid algorithm is given by:

$$M^{\mathrm{CGC}} = I - P\mathcal{L}_H^{-1}\bar{R}\mathcal{L}_h.$$

Error amplification operator of RK-schemes

- The amplification factor for the EXI Runge-Kutta-scheme is:

$$M_h^{\mathrm{EXI}} = \frac{I}{1+\alpha_5\lambda} + \frac{\alpha_5\lambda(I-\mathcal{L}_h)}{(1+\alpha_4\lambda)(1+\alpha_5\lambda)} + \cdots + \frac{\alpha_2\alpha_3\cdots\alpha_5(\lambda(I-\mathcal{L}_h))^4}{(1+\alpha_1\lambda)(\cdots)(1+\alpha_5\lambda)} + \frac{\alpha_1\alpha_2\cdots\alpha_5(\lambda(I-\mathcal{L}_h))^5}{(1+\alpha_1\lambda)(\cdots)(1+\alpha_5\lambda)}$$

- The amplification factor for the EXV Runge-Kutta-scheme is:

$$M_h^{\mathrm{EXV}} = I - \alpha_4\lambda\mathcal{L}_h + \alpha_3\alpha_4(\lambda\mathcal{L}_h)^2 - \cdots + \alpha_1\alpha_2\alpha_3\alpha_4(\lambda\mathcal{L}_h)^4$$

Coarse grid correction

- On a uniform grid, the prolongation operator defined becomes:

$$P \cong \left[\begin{array}{ccc|ccc|ccc} 1 & \frac{1}{2} & 0 & 1 & -\frac{1}{2} & 0 & 0 & 0 & 0 \\ 0 & \frac{1}{2} & 0 & 0 & \frac{1}{2} & 0 & 0 & 0 & 0 \\ 0 & 0 & 1 & 0 & 0 & 1 & 0 & 0 & 0 \end{array}\right]$$

- The right block is zero because the coarse grid element $\mathcal{K}_H^n = (x_{j-1}, x_{j+1}) \times (t^n, t^{n+1})$ corresponds to the fine elements $(\mathcal{K}_h^n)_L = (x_{j-1}, x_j) \times (t^n, t^{n+1})$ and $(\mathcal{K}_h^n)_D = (x_j, x_{j+1}) \times (t^n, t^{n+1})$.

- Note the block Toeplitz structure with 3×3 blocks; since $\bar{R} = P^T$ the restriction operator for the residuals is also block Toeplitz.

Stabilization term

- The parameter η has a significant effect on the stability of the Runge-Kutta methods: as η increases, the permissible pseudo-timestep decreases proportionally.
- Therefore η should be taken as small as allowed in the discontinuous Galerkin discretization, in general equal to the number of faces of an element.
- The convergence behaviour of the two-level algorithm for the space-time DG discretization is given by the spectral radius of the error amplification operator$\rho(M_h^{\mathrm{TLA}})$.

Fourier analysis of the two-level algorithm

- The eigenvalue spectra of the two-level algorithm and the eigenvalues of the Fourier transform $\widehat{M_h^{\mathrm{TLA}}}$ for $\omega \in [-\pi/H, \pi/H)$ are identical.

- The Fourier transform $\widehat{\mathcal{L}_h}$ of the block Toeplitz operator $\mathcal{L}_h$ is:

$$\widehat{\mathcal{L}_h}(\omega) = L_h e^{-\imath \omega h} + D_h + U_h e^{+\imath \omega h},$$

with $\imath = \sqrt{-1}$.

- Since the operators M_h^{REL}, P and $\bar{R}$ are also block Toeplitz, their Fourier transforms $\widehat{P}$ and $\widehat{\bar{R}}$ are computed similarly.

Stability parameters

- The space-time DG discretization is implicit in time and unconditionally stable.
- The Runge-Kutta methods are explicit in pseudo time and their stability depends on the ratio λ between the pseudo timestep and the physical timestep $\lambda = \Delta\tau/\Delta t$.
- The stability condition is expressed in terms of the pseudo-time CFL number $\sigma_{\Delta\tau}$ and the pseudo-time diffusive Von Neumann condition $\delta_{\Delta\tau}$:

$$\Delta\tau \leq \Delta\tau^a \equiv \frac{\sigma_{\Delta\tau} h}{a} \quad \text{and} \quad \Delta\tau \leq \Delta\tau^d \equiv \frac{\delta_{\Delta\tau} h^2}{d}.$$

  The pseudo-time CFL number is given by $\sigma_{\Delta\tau} = \lambda\sigma$ and the pseudo-time diffusive Von Neumann number by $\delta_{\Delta\tau} = \lambda\sigma/\mathrm{Re}_h$

Eigenvalue Spectra Two-Level Algorithm with EXI Smoother (Steady Case)

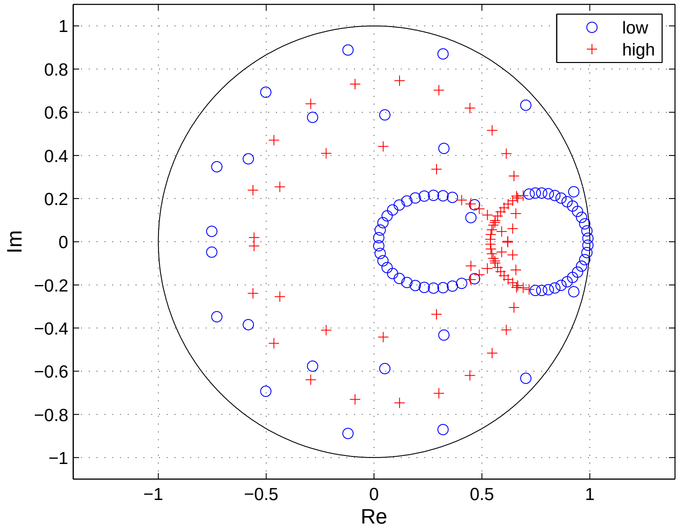

(a) EXI

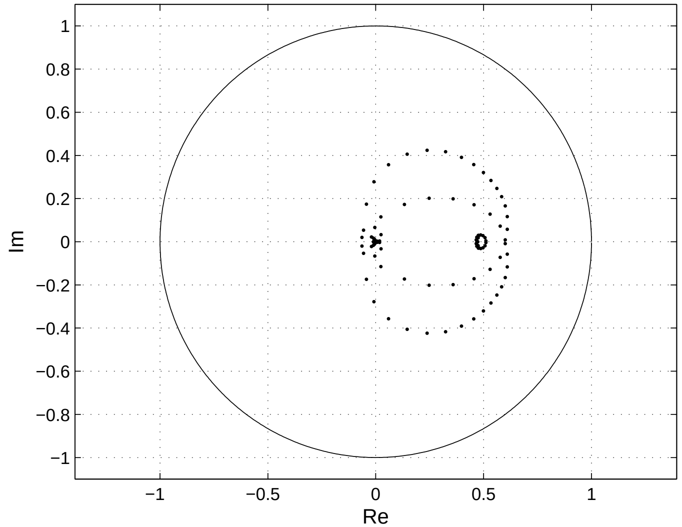

(b) TLA with EXI

Eigenvalue spectra of the EXI smoother and two-level algorithm in the steady advection dominated case ($\sigma = 100$ and $\mathrm{Re}_h = 100$).

Eigenvalue Spectra Two-Level Algorithm with EXV Smoother (Steady Case)

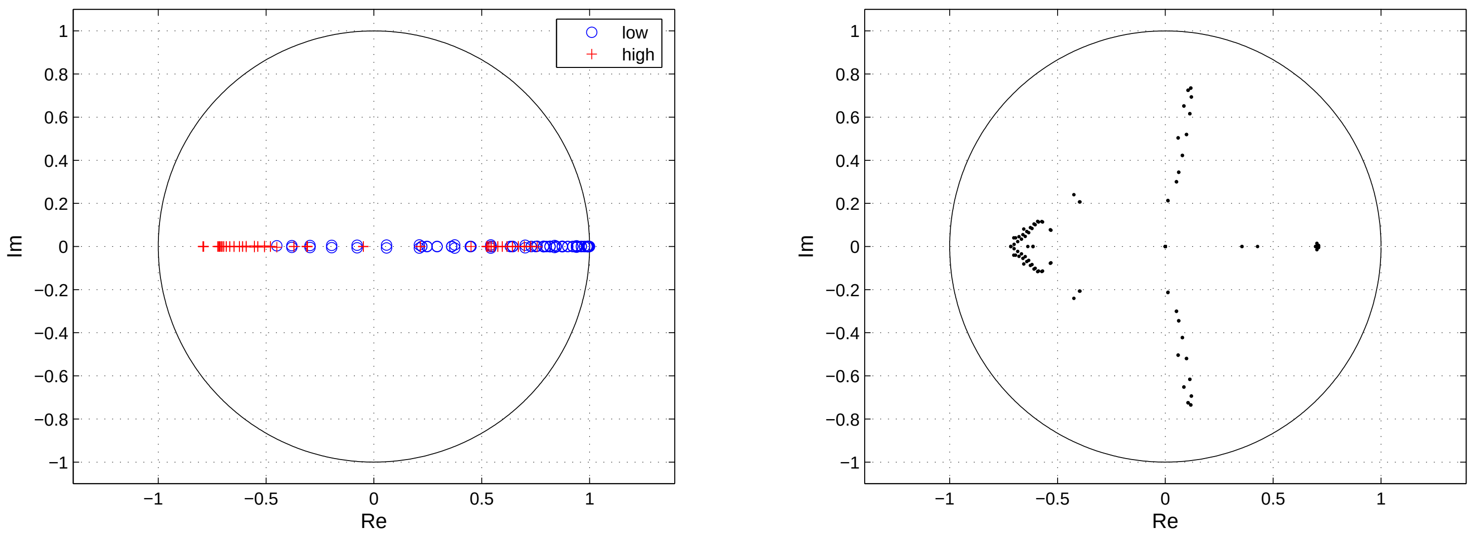

(c) EXI (d) TLA with EXI

Eigenvalue spectra of the EXV smoother and two-level algorithm in the steady diffusion dominated case ($\sigma = 100$ and $\mathrm{Re}_h = 0.01$).

Eigenvalue Spectra Two-Level Algorithm with EXI Smoother (unsteady case)

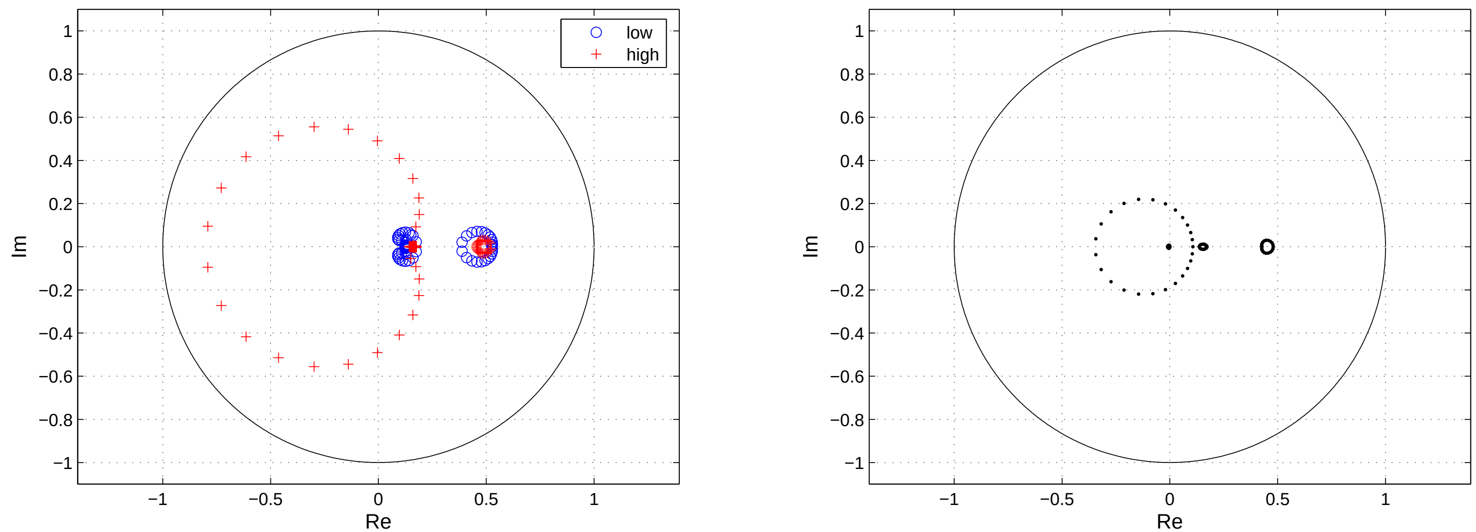

(e) EXI (f) TLA with EXI

Eigenvalue spectra of the EXI smoother and two-level algorithm in the unsteady advection dominated case ($\sigma = 1$ and $\mathrm{Re}_h = 100$).

Eigenvalue Spectra Two-Level Algorithm with EXV Smoother (unsteady case)

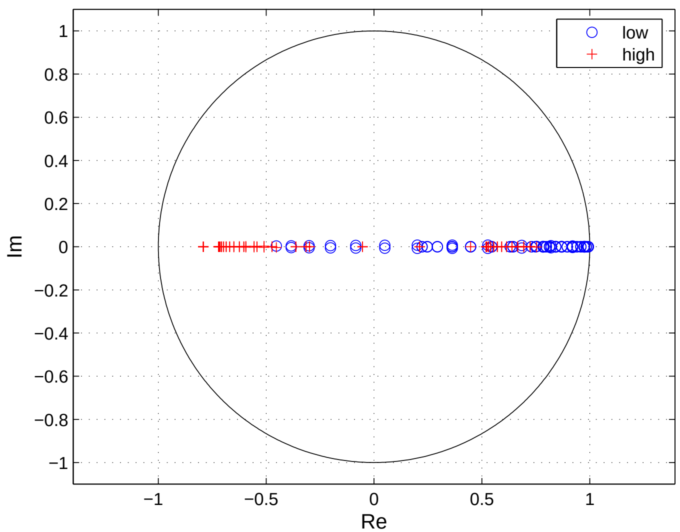

(g) EXI

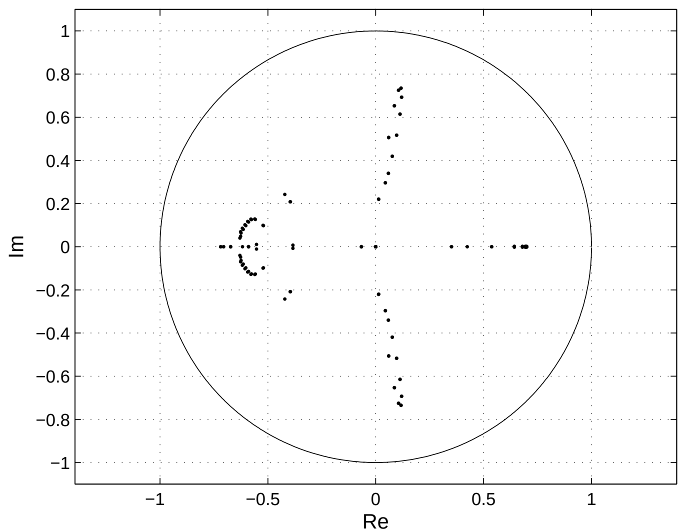

(h) TLA with EXI

Eigenvalue spectra of the EXV smoother and two-level algorithm in the unsteady diffusion dominated case ($\sigma = 1$ and $\mathrm{Re}_h = 0.01$).

Spectral Radii of Two-Level Algorithm for Steady Problems ($\sigma = 100$)

EXI smoother

Re_h	$\Delta\tau/\Delta t$	$\rho\left(M_h^{\mathrm{EXI}}\right)$	$\rho\left(M_h^{\mathrm{TLA}}\right)$
100	1.8e-02	0.991	0.622
10	8.0e-03	0.996	0.716
1	1.4e-03	0.999	0.906

EXV smoother

Re_h	$\Delta\tau/\Delta t$	$\rho\left(M_h^{\mathrm{EXV}}\right)$	$\rho\left(M_h^{\mathrm{TLA}}\right)$
100	2.0e-03	0.999	0.914
10	3.0e-03	0.998	0.871
1	7.0e-03	0.996	0.697

Spectral Radii of Two-Level Algorithm for Unsteady Problems ($\sigma = 1$)

EXI smoother

Re_h	$\Delta\tau/\Delta t$	$\rho\left(M_h^{\mathrm{EXI}}\right)$	$\rho\left(M_h^{\mathrm{TLA}}\right)$
100	1.6e-00	0.796	0.479
10	8.0e-01	0.918	0.599
1	1.4e-01	0.904	0.837

EXV smoother

Re_h	$\Delta\tau/\Delta t$	$\rho\left(M_h^{\mathrm{EXV}}\right)$	$\rho\left(M_h^{\mathrm{TLA}}\right)$
100	1.0e-00	0.924	0.660
10	7.0e-01	0.812	0.704
1	7.0e-01	0.805	0.719

First order discretization on the coarse grids

- For the space-time discontinuous Galerkin discretization of the Euler equations, constant basis functions were used on the coarse grids.
- This approach, however, is inadequate for the Navier-Stokes equations.

Spectral radii with first order discretization on coarse grids

physics		stability	convergence	
σ	Re_h	$\Delta\tau/\Delta t$	$\rho\left(M_h^{\mathrm{EXI}}\right)$	$\rho\left(M_h^{\mathrm{TLA}}\right)$
100	100	1.8e-02	0.991	0.979
1	100	1.6e-00	0.796	0.794

Spectral radii in the advection dominated cases.

physics		stability	convergence	
σ	Re_h	$\Delta\tau/\Delta t$	$\rho\left(M_h^{\mathrm{EXV}}\right)$	$\rho\left(M_h^{\mathrm{TLA}}\right)$
100	0.01	8.0e-05	0.999	0.998
1	0.01	8.0e-03	0.993	0.985

Spectral radii in the diffusion dominated cases.

Numerical simulations

- Definition of work units:
  - One work unit corresponds to one Runge-Kutta step on the fine grid.
  - The work on a one times coarsened mesh is $\frac{1}{8}$ of the work on the fine grid ($\frac{1}{4}$ in 2D).

Convergence Rate for Flow about a Circular Cylinder

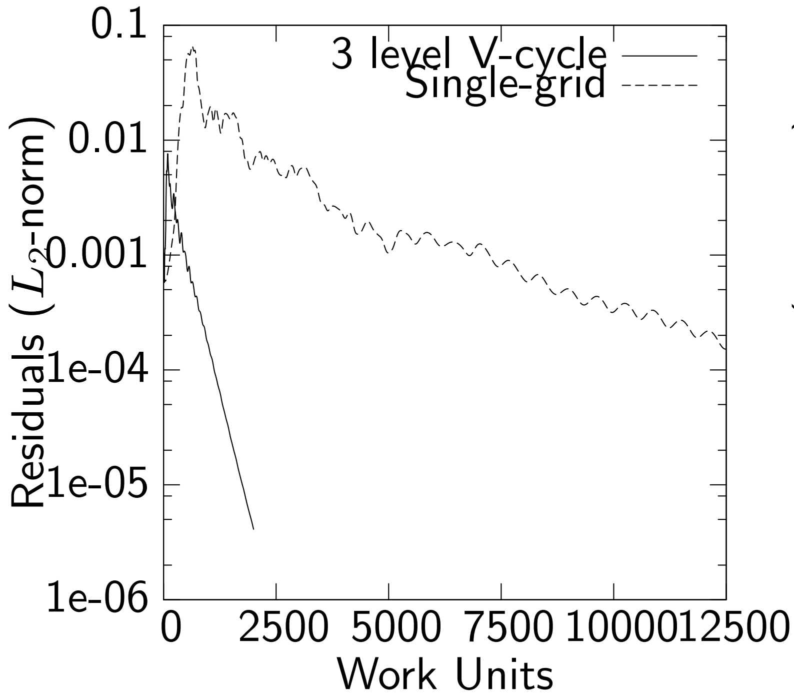

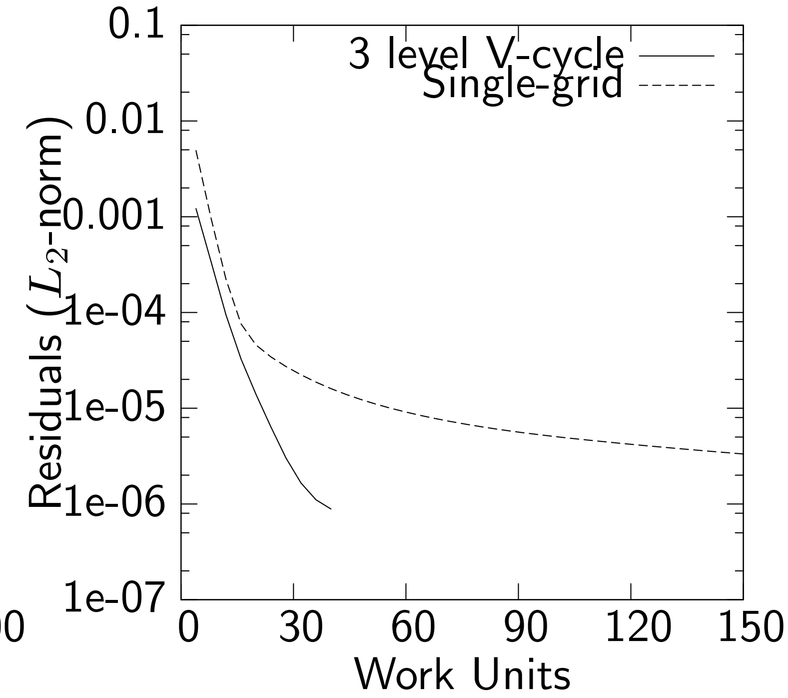

Steady-state (L) and time-accurate (R)

$\mathrm{M}_\infty = 0.3$, $\mathrm{Re}_\infty = 40$, 64×64 mesh (L) and 80×84 mesh (R)

Convergence Rate for Unsteady Flow about Circular Cylinder

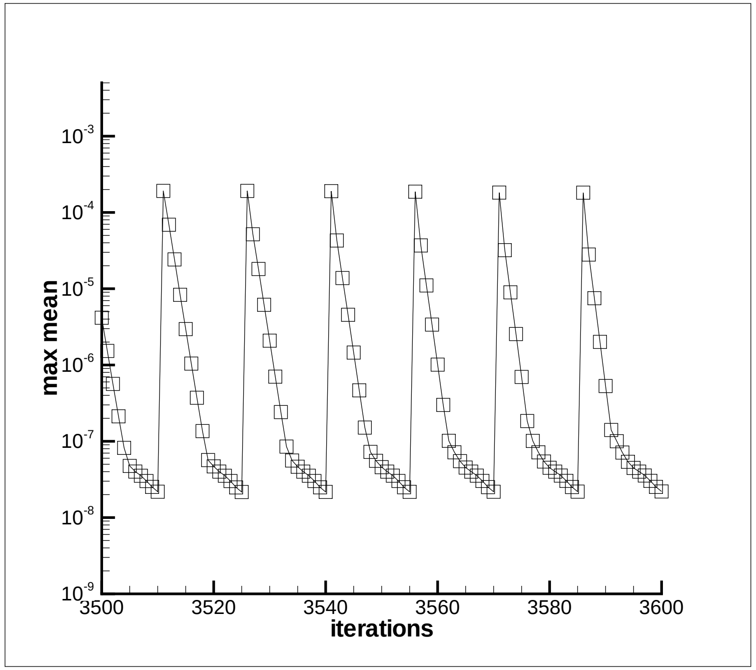

$M_\infty = 0.3$, $Re_\infty = 1000$ on a 128×128 mesh

Multigrid: 3 level V-cycle, 4 relaxation steps on each level.

Flow about ONERA M6 Wing

- Steady laminar flow about the ONERA M6 wing at $\mathrm{M}_\infty = 0.4$, $\mathrm{Re}_\infty = 10^4$ and angle of attack $\alpha = 1^\circ$.
- Fine grid consists of $125\,000$ hexahedral elements.
- Multigrid iteration consisting of 3 level V- or W-cycles.
- The V-cycle has a total of 4 relaxations on each grid level, while the W-cycle has 4 relaxations on the fine grid and 8 on the medium and coarse grid.

Convergence Rate for ONERA M6 Wing

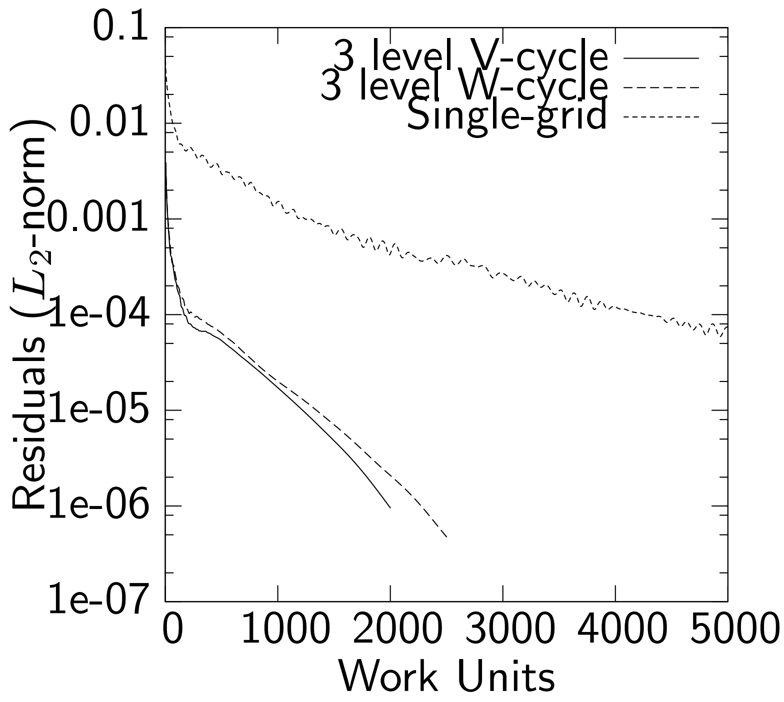

Convergence in pseudo-time for the ONERA M6 wing

$\mathrm{M}_\infty = 0.4$, $\mathrm{Re}_\infty = 10^4$, $\alpha = 1^\circ$.

Summary of Computational Effort for Different Cases

Case	Single-grid performance	Multigrid performance	Cost reduction
cylinder (steady)	2 orders in 12 500 WU	3 orders in 2000 WU	9.4
cylinder (unsteady)	3 orders in 150 WU	3 orders in 30 WU	5.0
ONERA M6	2 orders in 5000 WU	3 orders in 2000 WU	3.7

Summary of computational effort for cylinder and ONERA M6 wing.

Conclusions

The space-time discontinuous Galerkin method has the following interesting properties:

- Accurate, unconditionally stable scheme for the compressible Navier-Stokes equations.
- Conservative discretization on moving and deforming meshes which satisfies the geometric conservation law.
- Local, element based discretization suitable for h-(p) mesh adaptation.
- Optimal accuracy proven for advection-diffusion equation.

Conclusions

- The Taylor quadrature significantly improves the efficiency of the flux integrals without a reduction in accuracy.
- The use of a stabilization operator instead of a slope limiter makes it possible to converge to machine accuracy for steady state problems, whereas a limiter prevents convergence to steady state and reduces accuracy in a large part of the domain.
- Runge-Kutta pseudo-time integration methods in combination with multigrid are an efficient method to solve the nonlinear algebraic equations originating from the space-time DG method.

Conclusions

- Two-level Fourier analysis to the space-time DG discretization of the scalar advection-diffusion equation shows convergence factors between 0.62 and 0.74, which is quite good for a fully explicit multigrid algorithm.
- The construction of intergrid transfer operators is based on the L_2 projection of the coarse grid solution on the fine grid and assumes embedding of spaces.
- In practical computations the embedding of spaces is not very critical and no serious performance degradation is observed.
- Contrary to the Euler equations using a first order accurate discretization on the coarse meshes does not result in reasonable convergence rate.

More information on: `wwwhome.math.utwente.nl/~vegtjjw/`

References

1. L. Pesch and J.J.W. van der Vegt, A discontinuous Galerkin finite element discretization of the Euler equations for compressible and incompressible fluids, *J. Comput. Phys.*, **227**, pp. 5426-5446, 2008.

2. S. Rhebergen, O. Bokhove and J.J.W. van der Vegt, Discontinuous finite element methods for hyperbolic nonconservative partial differential equations, *J. Comput. Phys.*, **227**(3), pp. 1887-1922, 2008.

3. C.M. Klaij, M.H. van Raalte, H. van der Ven, and J.J.W. van der Vegt, h-Multigrid for space-time discontinuous Galerkin discretizations of the compressible Navier-Stokes equations , *J. Comput. Phys.*, **227**(2), pp. 1024-1045, 2007.

4. C.M. Klaij, J.J.W. van der Vegt and H. van der Ven, Pseudo-time stepping methods for space-time discontinuous Galerkin discretizations of the compressible Navier-Stokes equations, *J. Comput. Phys.*, **219**, 622-643 (2006).

5. C.M. Klaij, J.J.W. van der Vegt and H. van der Ven, Space-time discontinuous Galerkin method for the compressible Navier-Stokes equations, *J. Comput. Phys.*, **217**, 589-611 (2006).

6. J.J.W. van der Vegt and H. van der Ven, Space-time discontinuous Galerkin finite element method with dynamic grid motion for inviscid compressible flows. Part I. General formulation., *J. Comput. Phys.* **182**, pp. 546-585 (2002).

7. H. van der Ven and J.J.W. van der Vegt, Space-time discontinuous Galerkin finite element method with dynamic grid motion for inviscid compressible flows. II. Efficient flux quadrature, *Comput. Meth. Appl. Mech. Engrg.* **191**, pp. 4747-4780 (2002).

8. J.J. Sudirham, J.J.W. van der Vegt and R.M.J. van Damme, Space-time discontinuous Galerkin method for advection-diffusion problems on time-dependent domains, *Appl. Numer. Math.*, **56**(12), 1491-1518 (2006).

9. J.J.W. van der Vegt and J.J. Sudirham, A space-time discontinuous Galerkin method for the Time-Dependent Oseen Equations, article in print Appl. Numer. Math., 2007, doi:10.1016/j.apnum.2007.11.010.

10. J.J.W. van der Vegt and H. van der Ven, Discontinuous Galerkin finite element method with anisotropic local grid refinement for inviscid compressible flows, *J. Comput. Phys.* **141**, 46-77 (1998).